كلية الهندسة بشبرا
FACULTY OF ENGINEERING AT SHOUBRA
ERJ
PRINT ISSN 3009-6049
ONLINE ISSN 3009-6022

ENGINEERING RESEARCH JOURNAL (ERJ)
Volume (53) Issue (4)
October. 2024, pp: 98-105
https://erjsh.journals.ekb.eg

Assessment of Full-Scale Thin Wire Reinforced Concrete Beams

Asmaa Osama Ali Azab[1]*, Amr Ali Gamal EL-Din [2] ,Tarek Salah El-salakawy [2]

[1] Department of Civil Engineering, at High Institute of El-shourk , Cairo, Egypt
[2] Department of Civil Engineering, Faculty of Engineering at Shoubra, Benha University, Cairo, Egypt.
* Corresponding Author.
E-mail: asmaazab648@gmail.com,dr.amrgamal @hotmail.com tarek.abdelgalil@feng.bu.edu.eg.

Abstract: This research introduces a novel technique for reinforcing reinforced concrete (RC) beams by employing thin wire reinforcement bars of varying diameters (3mm, 4mm, 5mm, and 6mm), these steel thin wires which have small diameter from diameter (from 2mm to 8mm)(slender wires) have been proven to enhance stress distribution more effectively and enhance the bond strength between steel rebars and concrete by increasing the contact surface area between the two materials. Additionally, the percentage of the used bottom reinforcement for all beams remains constant at 100%, similar to the control beam, despite variations in the number of bars utilized in each beam, this alternative approach has the potential to significantly yield results. The research demonstrates a substantial improvement in beam strength through the utilization of thin wire rebars. The experimental investigation involved five full scale beams reinforced with mild steel rebar diameters. The results indicate that the tensile strength of reinforced concrete beams is influenced not only by the strength of the rebars but also by the surface area of the steel bars and their interaction with the concrete. Thin rebars exhibit superior flexibility and compatibility compared to larger diameter rebars. The experimental program yielded positive outcomes in terms of flexural capacity, deflection, ductility, and energy dissipation.

Keywords: Thin Wire Reinforcement; Ductility; Percentage of area steel; Bond; Surface area; Deflection; Experimental work; Energy dissipation & Flexural strength.

.

1. INTRODUCTION

An important new idea discusses reinforcing concrete using thin wire bars to study their effect on strength, deflection of concrete beams, crack pattern and failure modes. Previous studies focused on Steel wire-carbon-fiber reinforce(SCFR)plate as a novel way to strengthen concrete structures by combining carbon fiber with steel wire. It offers better ductility and lateral resistance together with the same tensile strength as traditional Carbon-fiber-reinforced plates (CFR)plates. SCFR plates also could reduce lateral strain. It has been shown through flexural testing that SCFR plates are more ductile than conventional CFR plates and increase in the load carrying capacity of [1-5]. The structural properties of plain concrete and fiber reinforced concrete using tested beams and prismatic specimens made with steel or polypropylene fibers were also investigated following RILEM guidelines, the tests focused on compressive and flexural tensile behavior and fracture energy. Results showed that adding fibers significantly improved the structural integrity and stability of concrete elements, thereby prolonging their service life. [6-11]. The author of this study presents a new mechanical model for polyvinyl alcohol fiber-reinforced ferrocement cementitious composite Polyvinyl alcohol fiber-reinforced ferrocement cementitious composite (PVA-RFCC), demonstrating integrated mechanical properties through polyvinyl alcohol(PVA) fiber reinforcement and steel wire mesh (SWM). Experiments and comparative analysis assess flexural toughness and the model is specifically designed for thin PVA-RFCC plates. The PVA fibers show exceptional behavior before peak strength, while SWM exhibits outstanding behavior after peak strength [12]. A new method to improve the strength of reinforced concrete

beams by combining Basalt fiber Reinforced Polymer Basalt Fiber Reinforced Polymer (BFRP) grid and Engineered Cementitious Composites (ECC) to form a composite reinforcement layer (CRL). The study found no debonding of the CRL, indicating the technique's effectiveness. Also, other research focused on analytical models developed for load-deflection predictions [13,14]. The mechanical performance of concrete, incorporating steel fibers with varying geometry and volume fraction, found that increasing the volume fraction of steel fibers in the concrete improved its toughness. The geometry of the fibers also significantly influenced the material's performance, as it was found that the addition of steel fibers enhanced the material's properties [15-18]. Researchers found that a wire mesh-epoxy composite significantly enhances the flexural strength and energy absorption of plain concrete beams. Wider composite widths showed better energy absorption, and the specific configurations of the composite also influenced the overall performance of the beams. [19-23].

2. Problem Statement

This research is focused on investigating the efficiency of the thin wire steel bars in reinforced concrete beams by distributing the total used area of steel bars to smaller bars in diameter and larger numbers of bars, which impacts the contact surface area of between steel bars and concrete, that lead to increase the flexural strength of reinforced beams and reduce the total concrete weight in matter of using smaller sections, as well as reduction of reinforcement amount and total coast.

3.Experimental Program

3.1Tested Specimen

The experimental program comprises of five full scale beam specimens, all having the same dimensions of (1750*300*150) mm. The reinforcement details, have been depicted in Figure 1, indicate that all beams posses identical top reinforcement bars of 2Ø6 and stirrups of 5Ø6/m. However, the bottom reinforcement varies among the five beams. The control beam, F5, has a bottom reinforcement of 2Ø8, while beams F1, F2, F3, and F4 have bottom reinforcement of 14Ø3, 8Ø4, 5Ø5, and 4Ø6 respectively and the number of bars in each beam has been carefully determined to maintain a consistent percentage of area srreinforcement in comparison to the control beam, which is set to 100%. The beam reinforcement and surface area are listed in Table.1.

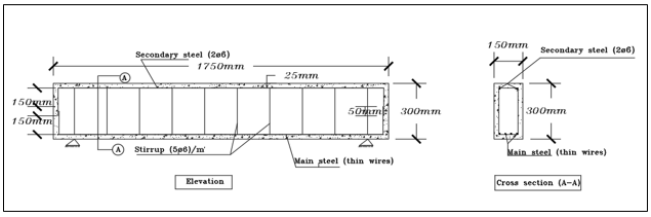

Fig .1 Schematic Details of Reinforcement of Beams.

Table .1. Specimens Reinforcement and Surface Area:

Beam	Bottom Reinforcement	Top Reinforcement	Stirrup (m`)	Area of Steel Bars (cm^2) at Bottom Side (Main Reinforcement)	Surface Area of Steel Bars (cm^2)	Surface Area of Beams / Surface Area of Control Beam.
F1	14 Ø 3	2 Ø 6	5 Ø 6	1.00	2638	263%
F2	8 Ø 4	2 Ø 6	5 Ø 6	1.00	2010	200%
F3	5 Ø 5	2 Ø 6	5 Ø 6	1.00	1570	156%
F4	4 Ø 6	2 Ø 6	5 Ø 6	1.00	1507	150%
F5	2 Ø 8	2 Ø 6	5 Ø 6	1.00	1005	100%

Table.2. Listed the Mix Proportions of Mortar:

Concrete Mix Componants	Weigth of m^3(Kg)					Additional
	Cement (kg)	Sand(Kg)	Gravel (1)(Kg)	Gravel (2)(Kg)	Water(Lit)	Sikament R -2004(Lit)
	400	710	540	580	175	5.5

Fig.2 Preparation of Concrete Standard Cubes

3.1 Sample Preparation and Test Setup

The preparation of the concrete beams involved various procedures, including the modification of the steel framework, wooden mold, and the pouring of the concrete mixture in accordance with the specified design mix,as depicted in Figure.3. Five concrete beam specimens underwent testing after a 28-day curing period to ascertain the intended strength of the concrete. The testing procedure entailed employing a 50-ton hydraulic jack in conjunction with three LVDTs to evaluate the displacement values of the beams. Furthermore, strain gages were affixed to the internal steel bars to gauge the strain of the specimens. steel, as illustrated in Figure 4.

Fig.3.Sample Preparations.

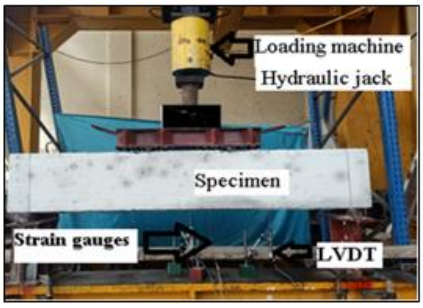

Fig .4. Test Setup

4.Experimental Result and Discussion

The results of the experimental program in terms of crack load, failure load and displacement are listed in Table .3. The control beam (F5) was reinforced with a steel diameter of 2Ø8 mm and a surface area of 1005 cm^2. Cracks occurred at a load of 12.65kN, extending from the bottom layer to the top layer, no local or combined failure was observed until the maximum ultimate load was reached at 55kN. The first beam with surface area of 2638 cm2 (F1) was reinforced with steel bars using 14Ø3, causing cracks at various loads, no local or shear failure was observed until a maximum load was reached to 81.37kN. The percentage of area steel in all beams were compared to the reference beam which was equivalent to100% of the control beam area of steel. The second beam (F2) was reinforced with steel bars8Ø4, with surface areas of 2010cm2. Cracks formed at different loads, reaching maximum load of 73.30kN. The third beam (F3) was reinforced with steel bars5Ø5, with a surface area steel of 1570 cm2. Cracks occurred at different loads, and several more occurred until the ultimate failure load of 65.70kN, was reached to the maximum loads. The fourth beam (F4) was reinforced with thin wire steel bars4Ø6, with surface area steel of 1507cm2. Cracks occurred at various loads, reaching ultimate failure loads of 69.47kN. The failure crack patterns are shown in Fig .5.

Table.3. Specimens Experimental Results.

Sample	Main Bottom Reinforcement	As (mm^2)	(As) Beams / (As) Reference	First Crack load (kN)	Failure Load (kN)	Avg. increase in Failure Load (%)	Max Displacement (mm)	Avg. increase in Displacement (%)
F1	14Ø3	100	100%	46.58	81.37	148%	10.70	134%
F2	8Ø4	100	100%	34.28	73.30	133%	10.21	128%
F3	5Ø5	100	100%	43.17	65.70	119%	11.00	138%
F4	4Ø6	100	100%	37.42	69.47	126%	10.60	133%
F5	2Ø8	100	100%	12.65	55.00	100%	8.00	100%

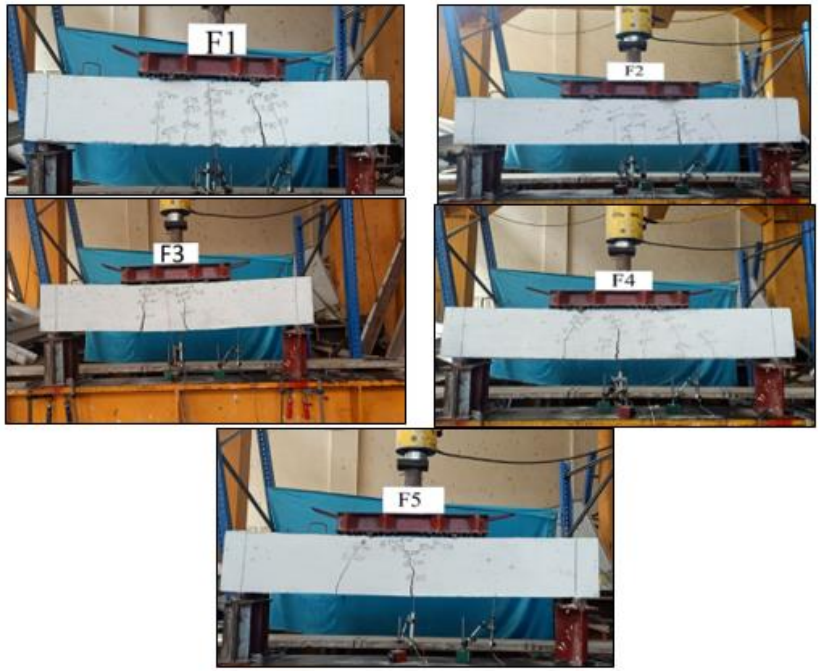

Fig.5. Crack Pattern for Beam Specimens

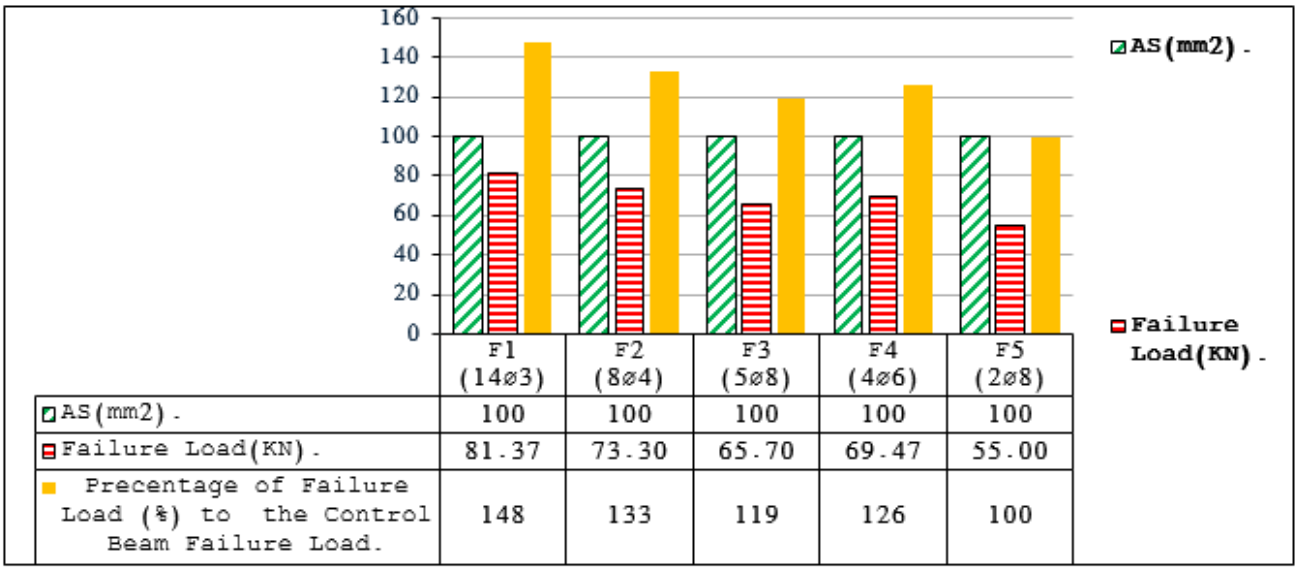

	F1 (14ø3)	F2 (8ø4)	F3 (5ø8)	F4 (4ø6)	F5 (2ø8)
AS(mm2).	100	100	100	100	100
Failure Load(KN).	81.37	73.30	65.70	69.47	55.00
Precentage of Failure Load (%) to the Control Beam Failure Load.	148	133	119	126	100

Fig .6. Failure Load &Area of Steel Bars.

4.1. Ultimate Load Discussion

The experimental findings indicate that there is a variation in the ultimate load when employing the same percentage of area steel but utilizing different diameters of steel bars. The outcomes of the beams are listed in Table 3 and in Figure.6, also presents these results. We can deduce some conclusion as follows, specimen (F5) with (2Ø8) was used as a reference. Comparing the results of beams with variable reinforcement diameters to the reference beam showed that the results of this comparison indicate the effectiveness of the use of small diameter bars and effectiveness of surface area of contact between smaller bars and the reinforced concrete matrix. Beams (F1, F2, F3, F4 and F5) have almost the same area of bottom reinforcement and failure load of (81.37, 73.30,65.70, 69.47 and55.00) kN, respectively. From this, we can conclude that keeping the same area of steel but distributing these areas in a much larger number of bars and a larger surface area of content can effectively increase the ultimate failure load by (148%,133%,119% and 126%) respectively, compared to the reference beam. The beams with identical bottom reinforcement area (100%) to the control beam (F5) exhibited ultimate failure loads of 81.37, 73.30, 65.70, and 69.47 kN, respectively. Enhancing the steel area to nearly (100%) in beams F1, F2, F3, and F4 led to a progressive rise in the ultimate load-carrying capacity by 148%, 133%, 119%, and 126% in comparison to the

baseline specimen (F5), as illustrated in Figure 6. The significance of utilizing the identical area steel but distributed using smaller diameters was emphasized in this study. This method effectively enhances the efficiency of the concrete matrix and increases the ultimate load carrying capacity when compared to the control beam. By adopting this approach, the overall strength of the concrete matrix can be improved.

4.2. Ductility of The Test Specimens

The connection between the load and displacement in the beams is strengthened by employing slender wires, as depicted in Figure 7. This curve ensures that a significant surface area of concrete is covered by the steel, resulting in a strong bond between the concrete and steel. Consequently, the concrete can bear the highest load at any given point of displacement across all beams. The assessment of a structure's seismic performance heavily depends on its ductility. The ductility factor, defined as the ratio of the maximum displacement (D max) to the yield displacement (D yield) of the structure, which a critical parameter in this evaluation. The use of an ideal bilinear curve, with the yield displacement located at the intersection of the elastic and inelastic regions, offers a reliable approach to determine the yield displacement. In this study, the ASTM E126 [25] method was utilized to establish the bilinear curve of the specimen. Following a similar procedure, the intersection point of the envelope curve and hyperbolic curve should be at a distance greater than or equal to 0.4 Pmax, and they should coincide until reaching the limit displacement. At 0.8 Pmax bearing capacity, the displacement on the envelope curve of the specimen is considered as the displacement of the equivalent bilinear curve. The bilinear curve of each specimen was determined to be equal to the average value obtained from the push-pull envelope curve, as illustrated in Figure.8 and Figure.9. The factors considered for calculating the specimens' ductility coefficient are listed in Table.4. The test results indicated a significant increase in ductility for each beam specimen compared to the control beam F5.

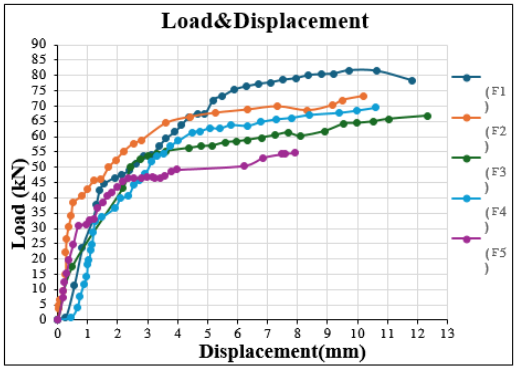

Fig .7. Explain Relation Between Load and Displacement

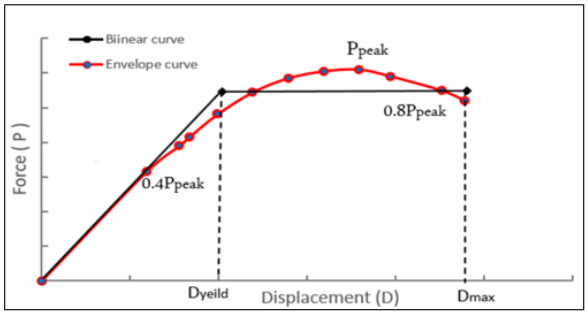

Fig.8. Specimen Bilinear Curve**.**

Bilinear Versus Envelope Load– Displacement Curve Average Idealized Bilinear Curves for the Specimens**.**

The general trend indicates that as the surface area of steel bars increases the ductility coefficient percentage showed a continuous increase which was attributed to the increased ductility associated with the increase in surface area of steel bars. This trend was observed in all groups. It was also noted that the best performance achieved regarding ductility coefficient percentage was in beams (F1, F2&F4) which showed an increase in ductility coefficient percentage by (134%,132%&142). For (5mm) bars the ductility coefficient percentage decreased to (129%) for (F3) which was distributed to decrease in surface area of steel. these results were compatibility with energy dissipation results.

Table .4. Displacements in the Bilinear Curves and the Ductility Values

Specimen	Yield Displacement. Average (mm)	Limit Displacement. Average (mm)	Ductility Coefficient μ	Increased ductility Coefficient (%)
F1	1.50	10.70	7.13	134%
F2	1.45	10.21	7.04	132%
F3	1.60	11.00	6.88	129%
F4	1.40	10.60	7.57	142%
F5	1.50	8.00	5.33	100%

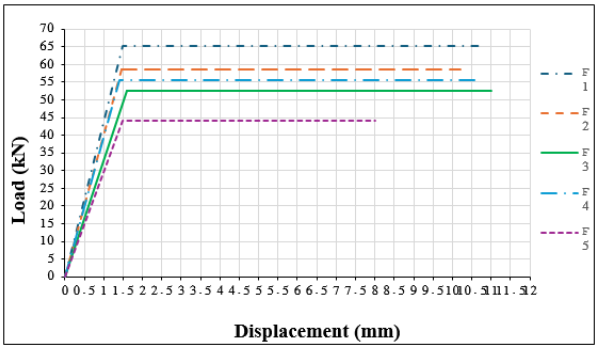

Fig. 9. Specimen Bilinear Curve.

4.3. Energy Dissipation

Energy dissipation is defined as the area under the load displacement curve, in our study it based on the area under the curve revealed that enhancement the specimen's ability to dissipate energy was clearly impacted by the change in reinforcement steel diameter which list in Table .5. When the surface area of steel increased with respect to reference beam (F5) the total energy dissipation showed a continues increased, this trend is observed in all beams. This was attributed to increased ductility in reinforced concrete beams associated with an increase in surface area steel bars. The best performance achieved was that encountered in (F1, F2 and F4) with an energy dissipation of (172, 165 and 161%) which indicates that (F1) with(3mm) bars and (F2) with (4 mm) bars and (F4) with (6mm) show a very good correlation between compatibility of the reinforcement steel with the concrete matrix and the effectiveness of surface area of steel when using these diameters. This was especially noted in the case of (F1). In the case of (F3) the energy dissipation started to decrease to reach a maximum of (150%) only due to decrease in surface area of steel.

Table .5. Energy Dissipation.

Specimen	Total Energy Dissipation (kN.mm)	Increase Total Energy.Dissipation (%)
F1	561.03	172%
F2	536.78	165%
F3	489.26	150%
F4	524.67	161%
F5	325.94	100%

5. Analytical Solution

The correlation between stress and strain for the materials employed in the experimental study, along with the comprehensive cross-section modeled in accordance with CEB-FIP guidelines [26,27], is illustrated in Figure 10 and Figure 11.

Within the compression zone, the height x is divided into n equal segments, with each segment denoted as hi. The calculation of hi is based on the guidelines established by the Egyptian Code (ECP 203-2018) [24].

$$hi = \frac{h}{n} \quad (1)$$

For every specified strain Ɛb of the concrete, an initial height value x is postulated, representing the distance from the outermost edge of the concrete under compression to the neutral axis. Utilizing the premise of a flat cross-section, the strain for each segment of the concrete, denoted as Ɛi, is calculated accordingly.

$$Ɛi = \frac{\boldsymbol{x - xi}}{\boldsymbol{x}} Ɛb \quad (2)$$

Table . 6. Characteristic values used in the stress–strain model.

Concrete	Steel
fcu = 32.71 MPa	fy = 200 MPa
Ɛc0 = 0.002	$Ɛs_0$ =0.001
Ɛcu = 0.035	Ɛcu =0.025
Ɛct0 =	
b = 150mm	

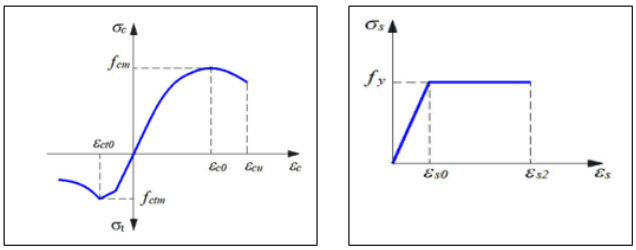

Fig. 10. Stress–strain relationship of materials used in the calculation.

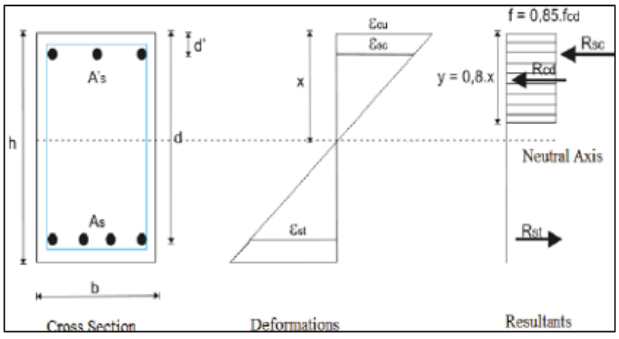

Fig 11. D In this context, xi represents the distance measured from the edge of the concrete under compression to the centroid of the concrete element, as detailed below:

$$xi = (i - 0{,}5)hi \quad (3)$$

Under the assumption that the concrete exhibits an ideal bond with the reinforcement and disregarding the role of concrete in the tensile region, the deformation values for

both compressive and tensile reinforcement can be calculated using Equations (4) and (5), respectively.

$$\varepsilon s* = \frac{x - hs*}{x} \varepsilon b \quad < \quad \varepsilon s0 \qquad (4)$$

$$\varepsilon s = \frac{hs - x}{x} \varepsilon b \quad < \quad \varepsilon s0 \qquad (5)$$

where hs and hs* are the distances from the edge of the concrete in compression zone to the centroid of the tensile reinforcement and compressive reinforcement respectively. The stress s_{bi} of the concrete element may be determined based on the stress and strain relationship equation of concrete. The resultant force of concrete in compression zone C is determined by using Equations (6):

$$C = \sum_{i=1}^{n} \sigma_{bi}\, bh_i \qquad (6)$$

Tensile force Ts in tensile reinforcement and Ts* in compressive reinforcement determined using Equations (7)–(8):

$$Ts = Es\, \varepsilon s\, As \qquad (7)$$

$$Ts* = Es\, \varepsilon s*\, As* \qquad (8)$$

where As, As*are the area of tensile reinforcement and compressive reinforcement respectively. Resulting in the Equation (9) or (10) of equilibrium force balance according to the Egyptian Code (ECP 203-2018) [24]:

$$C + Ts* = Ts \qquad (9)$$

OR

$$\sum_{i=1}^{n} \sigma_{bi}\, bh_i + Es\, \varepsilon s*\, As* = Es\, \varepsilon s\, As \qquad (10)$$

The height x corresponding to each compression strain εb can be determined from Equation (11) by iteratively modifying x until the expression C + TS* - TS is less than 10^{-6}. Subsequently, the bearing capacity of the cross-section is calculated using:

$$M_U = T_S\left(h_s - \frac{x}{2}\right) + T_S*\left(h_s* - \frac{x}{2}\right) \qquad (11)$$

Table .7 illustrates the likely extent of alignment between the theoretical and experimental findings in this research.

Table. 7. Comparison of theoretical and experimental results for the critical moment calculation.

Test Specimen	Theoretical Results(kNm)	Experimental Results(kNm)	Deviation (%)
F1	24.50	27.50	12.24
F2	26.30	24.74	5.93
F3	27.52	22.17	19.43
F4	29.10	23.45	19.42
F5	27.31	18.56	32.02

6. Conclusion

The study focused on examining the behavior of beams that were reinforced with smaller diameter of steel bars. The main objective of the research was to analyze and contrast the behavior of beams that were reinforced with varying diameters of steel but had the same area of steel. The study provided an overview of the substitution of steel bars, which are typically used as the primary reinforcement in steel beams, with different types of thin diameter bars. Additionally, it discussed the different methodologies employed to investigate various factors and parameters that influence the behavior of reinforced beams, such as load carrying capacity, deflection, ductility, and energy dissipation. Through an experimental program, the research evaluated the effectiveness of using thin-wire steel reinforcement and its impact on the behavior of concrete beams. The findings illustrated the behavior of concrete beams from the initial stages of loading to the point of maximum failure load, along with the corresponding deflection observed in the concrete beams. The five specimens demonstrated the capability of thin wire bars in beams to dissipate energy, as well as improving load carrying capacity and ductility. The deduced conclusions are listed below.

1- The use of same area of steel for the tested beams with respect to reference beam resulted in (148%,133% ,126&119%) increase in strength in (F1, F2, F3and F4) with a diameter of (3mm, 4mm,5mm and 6 mm) which could have a significant economic impact.
2- When comparing (F1, F2, F3and F4) deflection to the control beam (F5) it has been noted that the deflection increased by (34%,28%38% and 33%) respectively in beams compared control beam which indicates increased ductility & NO. of cracks.
3- The best performance achieved was that of (100%) area steel where the ultimate load carrying capacity for (F3) reached (119%) for ø5mm bars and increased to (133%) for ø4mm bars in (F2) and reached a maximum of (148%) in the ultimate load carrying capacity of (F1) ø 3mm bars.
4- The percentage of area steel increases the ductility co-efficient percentage increases this trend was observed in all beams due to increased ductility in (F1, F2, F3 and F4) ductility coefficient percentage increased to reach (134%,132%,129% and 142%).
5- The general trend shows that energy dissipation showed continuous increase as the no. of bars increased. This trend was observed in all beams. Energy dissipation levels were shown in (F1, F2, F3&F4) reached a maximum of (172%) in beam (F1).

6- The analytical solution indicates that the ratio of theoretical to experimental beams is probably accepted with approximately diversion of 25%.

Reference

[1]. Zhu, Wanxu, et al. "Behavior of RC Beams Strengthened Using Steel-Wire–Carbon-Fiber-Reinforced Plates." Materials 13.18 (2020): 3996.

[2]. de Montaignac, R., Massicotte, B., and Charron, J. (2012). "Design of SFRC structural elements: Flexural behavior prediction." Mater. Struct., 45(4), 623–636.

[3]. Toutanji, H., Zhao, L., & Zhang, Y. (2006). Flexural behavior of reinforced concrete beams externally strengthened with CFRP sheets bonded with an inorganic matrix. Engineering structures, 28(4), 557-566.

[4]. Esfahani, M. R., Kianoush, M. R., & Tajari, A. R. (2007). Flexural behaviour of reinforced concrete beams strengthened by CFRP sheets. Engineering structures, 29(10), 2428-2444.

[5]. Barros, Joaquim AO, and Joaquim A. Figueiras. "Flexural behavior of SFRC: testing and modeling." Journal of materials in civil engineering 11.4 (1999): pp331-339.

[6]. Bencardino, Francesco, et al. "Experimental evaluation of fiber reinforced concrete fracture properties." Composites Part B: Engineering 41.1 (2010): 17-24.

[7]. Sahoo, Dipti Ranjan, Apekshit Solanki, and Abhimanyu Kumar. "Influence of steel and polypropylene fibers on flexural behavior of RC beams." Journal of Materials in Civil Engineering 27.8 (2015): 04014232.

[8]. Li, Jun, Chengqing Wu, and Zhong-Xian Liu. "Comparative evaluation of steel wire mesh, steel fiber, and high-performance polyethylene fiber reinforced concrete slabs in blast tests." Thin-Walled Structures 126 (2018): pp117-126.

[9]. Banthia, Nemkumar, and Rishi Gupta. "Influence of polypropylene fiber geometry on plastic shrinkage cracking in concrete." Cement and concrete Research 36.7 (2006): 1263-1267.

[10]. Patel, P. A., Desai, A. K., & Desai, J. A. (2012). Evaluation of engineering properties for polypropylene fibre reinforced concrete. International Journal of Advanced Engineering Technology, 3(1), 42-45.

[11]. Hsie, M., Tu, C., & Song, P. S. (2008). Mechanical properties of polypropylene hybrid fiber-reinforced concrete. Materials Science and Engineering: A, 494(1-2), 153-157.

[12]. Du, W., Yang, C., Wang, C., Pan, Y., Zhang, H., & Yuan, W. (2021). Flexural behavior of polyvinyl alcohol fiber–reinforced ferrocement cementitious composite. Journal of Materials in Civil Engineering, 33(4), 04021040.

[13]. Zheng YZ, Wang WW, Brigham JC. Flexural behavior of reinforced concrete beams strengthened with a composite reinforcement layer: BFRP grid and ECC. Constr. Build. Mater. 2016; 115: 424–37.

[14]. Hou, W., Li, Z. Q., Gao, W. Y., Zheng, P. D., & Guo, Z. X. (2020). Flexural behavior of RC beams strengthened with BFRP bars reinforced ECC matrix. Composite Structures, 241, 112092.

[15]. Bencardino, F., Rizzuti, L., Spadea, G., & Swamy, R. N. (2010). Experimental evaluation of fiber reinforced concrete fracture properties. Composites Part B: Engineering, 41(1), 17-24.

[16]. Soulioti, D. V., Barkoula, N. M., Paipetis, A., & Matikas, T. E. (2011). Effects of fibre geometry and volume fraction on the flexural behaviour of steel-fibre reinforced concrete. Strain, 47, e535-e541.

[17]. Hamrat, Mostefa, et al. "Experimental study of deflection of steel fibre reinforced concrete beams: comparison of different design codes." European Journal of Environmental and Civil Engineering (2020): 1-17.

[18]. Chunxiang, Qian, and Indubhushan Patnaikuni. "Properties of high-strength steel fiber- reinforced concrete beams in bending." Cement and Concrete Composites 21.1 (1999): pp 73-81.

[19]. Qeshta, I. M., Shafigh, P., Jumaat, M. Z., Abdulla, A. I., Alengaram, U. J., & Ibrahim, Z. (2014). Flexural behaviour of concrete beams bonded with wire mesh-epoxy composite. Applied Mechanics and Materials, 567, 411-416.

[20]. Al Saadi, H. S. M., Mohandas, H. P., & Namasivayam, A. (2017). An experimental study on strengthening of reinforced concrete flexural members using steel wire mesh. Curved and layered structures, 4(1), 31-37.

[21]. Chandramouli, P., Muthukrishnan, D., Sridhar, V., Sathish Kumar, V., Murali, G., & Vatin, N. I. (2022). Flexural behaviour of lightweight reinforced concrete beams internally reinforced with welded wire mesh. Buildings, 12(9), 1374.

[22]. Maraq, M. A. A., Tayeh, B. A., Ziara, M. M., & Alyousef, R. (2021). Flexural behavior of RC beams strengthened with steel wire mesh and self-compacting concrete jacketing—experimental investigation and test results. Journal of materials research and technology, 10, 1002-1019.

[23]. Pan, Yuan. "Flexural behavior of reinforced concrete beams strengthened with steel wire mesh and polymer mortar." Advanced Materials Research. Vol. 250. Trans Tech Publications Ltd, (2011).

[24]. ECP Committee. (2018). Egyptian Code for Design and Construction of Concrete Structures (ECP 203-2018). Housing and Building National Research Center: Cairo, Egypt.

[25]. Energy based procedure to obtain target displacement of reinforced concrete structures - Scientific Figure on ResearchGate. Available from: https://www.researchgate.net/figure/Capacity-and-bilinear-curves_fig2_259601682 [accessed 23 Mar 2024].

[26]. Code, Model. "fib model Code for concrete structures." Structural Concrete 14 (2010).

[27]. Nguyen, Trung Hieu, Van Tuan Nguyen, and Minh Tuan Phan. "Experimental study on the flexural behaviour of corroded concrete beams reinforced with hybrid steel/GFRP bars." Structure and Infrastructure Engineering 20.6 (2024): 834-845.